

# The Experimental Analysis of the Burning Characteristics of Electrically Controlled Solid Propellant

Daehong Lim<sup>1</sup>, Kanagaraj Gnanaprakash<sup>2</sup>, Rajendra Rajak<sup>1</sup>, Jack J. Yoh<sup>1\*</sup>

<sup>1</sup>Department of Aerospace Engineering, Seoul National University, Seoul, 08826, Republic of Korea

<sup>2</sup>Department of Mechanical and Aerospace Engineering, Indian Institute of Technology Hyderabad, Kandi, Telangana, 502284, India

## Abstract

Electrically controlled solid propellant (ECSP) system has been introduced due to its potential in thrust regulation. However, the type of metal additives in ECSP directly affects the burning rate of the propellant thereby the thrust. Present study investigates the burning characteristics of two metalized samples composed of electrically controlled solid propellant combined with 5% (M5) and 15% (M15) (%wt) Tungsten (W) as metal additive. The burning characteristics of ECSP with addition of tungsten was studied through electric signal, flame temperature, and high-speed images. From the electric signal analysis, the two distinct regions were observed: the transient and steady regions. In the transient region, the current and voltage remained almost constant, whereas in the steady region, the current increased linearly for both the metalized samples. When the ongoing burning process belonged to the transient region, intermittent burning was detected, whereas when the process belonged to the steady region a steady downward burning was observed. The flame temperature for both the sample exhibited different burning characteristics, for instance a higher power was required to maintain the combustion of M5 sample, and the flame temperature of the sample was higher. However, as the metal content increased by 15% (M15), the flame temperature decreased by 9%. This is because of the change in metal oxidation with increase in metal content in baseline composition of ECSP. Further it is observed that, the exothermic reaction temperature range of the M5 sample was narrower than that of M15. Therefore, it could be inferred that the increase in metal content in ECSP could cause a transition in the burning characteristics due to its molecular characteristics.

## 1 Introduction

Inability to regulate thrust have been considered as a significant weakness of conventional solid propellant systems compared to the liquid propellant systems. Meanwhile, the solid propellant system has an irreplaceable advantage due to its excellent storage characteristics and wide range of military and civilian applications [1]. In recent years, electrically controlled solid propellants (ECSPs) have been gaining continuous interest in overcoming the shortcomings of conventional solid propellants. ECSPs have a unique operational advantage of multiple start/stop during the operation over conventional solid propellant. Similar to conventional solid propellant, ECSPs have a great

storing characteristic and is able to operate quickly. Moreover, ECSP burns only when external electric power is applied. Thus, the regulation of the thrust can be easily achieved.

Due to the high potential of ECSPs in different domains of application, researchers are already working and conducting experiments to further improve the performance of the ECSP-based propellant system. Sawka et al. [2] investigated the burning characteristics of ammonium nitride (AN) and hydroxyl ammonium nitrate (HAN)-based ECSPs. Glascock et al. [3] studied the burning and thrust characteristics of polytetrafluorethylene (PTFE)-based ECSPs. Zamir et al. [4] investigated the effects of change in pressure and applied voltage on the burning characteristics of AN-based ECSPs. Gobin et al. [5] examined the variation of compositional effects on the propellants by changing the contents of polyethylene oxide (PEO), lithium perchlorate (LP), and ammonium perchlorate (AP).

Recently, HAN-based ECSPs have been widely studied due to its low toxicity. Bao et al. [6] investigated the burning characteristics of HAN-based ECSP, such as ignition delay, burning rate and burning behavior, from ignition to extinction of flame. He et al. [7] revealed the decomposition characteristics of by using thermal analysis. Hiatt et al. [8] analyzed the flame sensitivity against the flame.

However, HAN-based ECSPs faces challenges due to hygroscopicity, and LP based ECSPs have been investigated to overcome this challenge. In order to avoid this challenge, the LP-based ECSPs have been introduced. Gnanaprakash et al. [9] investigated the decomposition characteristics of LP-based ECSPs via several measurement techniques. Li et al. [10] analyzed the effect of electrode materials on burning characteristics. In addition, optical multi-wavelength pyrometry was adopted in this study to measure the flame temperature. Weismiller et al. [11] measured the temperature distribution of aluminum (Al)-containing nano-thermite with two types of pyrometry.

In the present study, the burning characteristics of ECSP have been analyzed by various measurement techniques. Thus, the phase transition could be detected during the burning procedure. The study focused on the confirm the burning characteristics before and after the transition time. Therefore, electric signal measurement, optical pyrometry, high-speed imaging, and thermal analysis of the ECSPs which had different metal content were to understand the effect of the parameters on burning characteristics.

## 2 Methodology

---

\*Corresponding author, Fax: +82-02-882-1507  
E-mail address: [jjyoh@snu.ac.kr](mailto:jjyoh@snu.ac.kr) (J.J. Yoh)

## 2.1 Propellant sample

In the present study, two different type of samples were prepared which consists of 5% and 15% Tungsten (W, US Research Nanomaterials Inc., particle size of 1  $\mu\text{m}$ ) as a metal additive combined with baseline composition of ECSP. Two samples (M5 and M15) were prepared by changing the ratio of LP and H<sub>2</sub>O, keeping the rest of the ingredients unaltered. Detailed compositions of the samples were listed in Table 1. The ratio between LP and H<sub>2</sub>O was fixed as 1.85 because of solubility. Here, LP (Alfa Aesar Ltd., 99% purity) and polyvinyl alcohol (PVA, Sigma-Aldrich Ltd., >99% hydrolyzed, molecular weight of 146,000–186,000) were used as oxidizer and fuel, respectively.

Table 1: Compositions of the samples.

| (wt%)                          | M5<br>(5%-metalized) | M15<br>(15%-metalized) |
|--------------------------------|----------------------|------------------------|
| H <sub>2</sub> O               | 50.63                | 44.14                  |
| LP                             | 27.37                | 23.86                  |
| PVA                            | 10                   | 10                     |
| W                              | 5                    | 15                     |
| Glycerol                       | 5                    | 5                      |
| H <sub>3</sub> BO <sub>3</sub> | 2                    | 2                      |

## 2.2 Experimental setup

Figure 1 shows the schematic of the experimental setup used in this study. Samples were placed on the test stand which was directly connected to the power supply (1 kV and 1 A). Each of positive and negative electrodes were connected to the top and bottom surfaces of the sample, respectively. The electrodes were made of molybdenum (Mo) that had a 2896 K of melting point which was higher than the flame temperature. Two oscilloscopes (Tektronix, TBS 1052B-EDU, 50 MHz bandwidth, 1 GS/s sampling rate and Teledyne, WaveSurfer 3104z, 1 GHz bandwidth, 4 Gs/s sampling rate) were used to obtain the data from voltage probe (Hantek, T3100), current probe (Tektronix, A622), spectrometer (Dongwoo Optron, MonoRa320i), and intensified charge-coupled device (ICCD, Andor, iStar) for high speed imaging. A pyrometer consisting of an achromatic doublet lens (Thorlabs, MAP10100100-A, 400–700 nm) and fiber optics (Ocean Optics, QP200-2-UV-BX, 200  $\mu\text{m}$  diameter) which was used to obtain the flame spectrum. Here, the intensity of the equipment was calibrated before the measurements of flame spectrum. Thermal analyses are performed by using differential scanning calorimetry (DSC, Mettler Toledo, DSC 3+) and thermogravimetric analysis (TGA, Mettler Toledo, TGA 2) with temperature heating range of 30–600°C and N<sub>2</sub> flow rate of 40 ml/min.

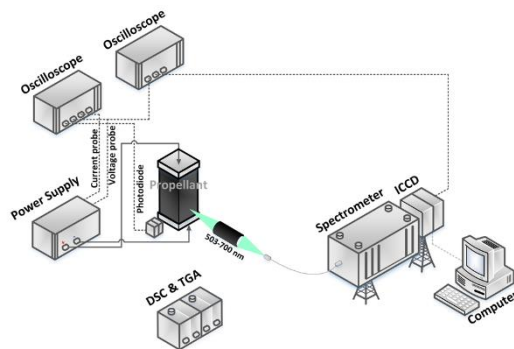


Figure 1: Schematic of the experimental setup

## 3 Results

### 3.1 Burning sequences

Figure 2 shows the electric signals during the overall burning process of the two samples. The difference in electric signals in the transient and steady regions are clearly observed. It is observed that, as soon as the external electric potential reaches 300 V, the internal current increases immediately and reaches a maximum value for both the samples at location A (Fig. 2(a)). The regions between A and B is regarded as transient region in which the internal current maintained at constant level whereas the voltage shows a transition. At location B, the current decreased whereas the voltage increased drastically. In the region B to C, the internal current exhibited a linear whereas the voltage remained constant. The observations were similar for both the samples.

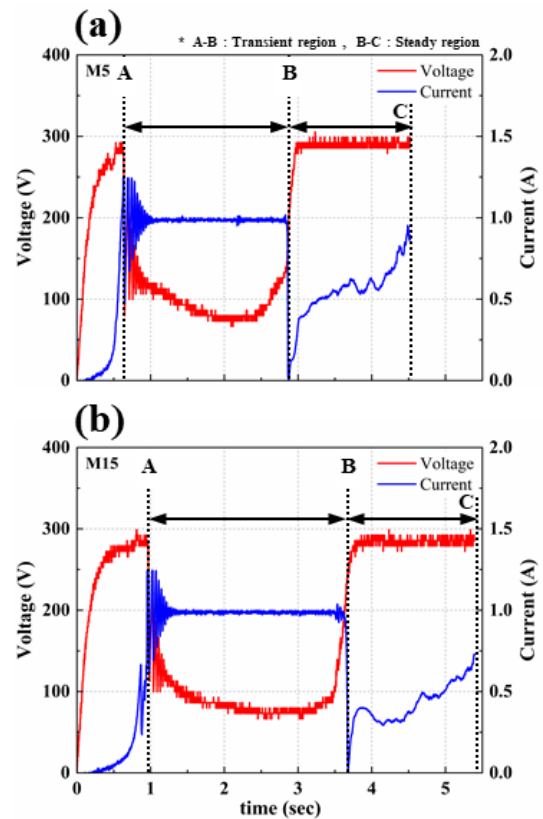


Figure 2: Electric signals of (a) M5 and (b) M15 during burning.

Figure 3 shows the sequential high-speed image of M5 burning in steady and transient regions. The reference image showing the raw ECSP (M5) is shown in Fig. 3 (a). In transient region, the propellant was burned intermittently. This indicates at transient region, only short-lived flames at single or various points existed (Fig. 3(b)). The flame could be observed at the rear surface of the propellant with no significant decrease in propellant length indicating inconsistency in flame generation. At this region the flames generated on the random positions and extinguished within a short time span. Meanwhile, in the steady region, a gradual regression of propellant was accompanied by uniform

burning (see Fig. 3(c)). During the steady burning the length of the propellant continuously decreased and the burning occurred at the interface between top surface of propellant and the electrode as shown in Fig. 3 (c). Moreover, this type of flame was maintained during the overall steady region, and the tendency to show a uniform burning rate was remarkable. Unlike the flame observation at irregular points on the front and rear surface of propellants in the transient region, in the steady region a consistent flame within a limited area, in between the interface of the propellant and the positive electrode was observed.

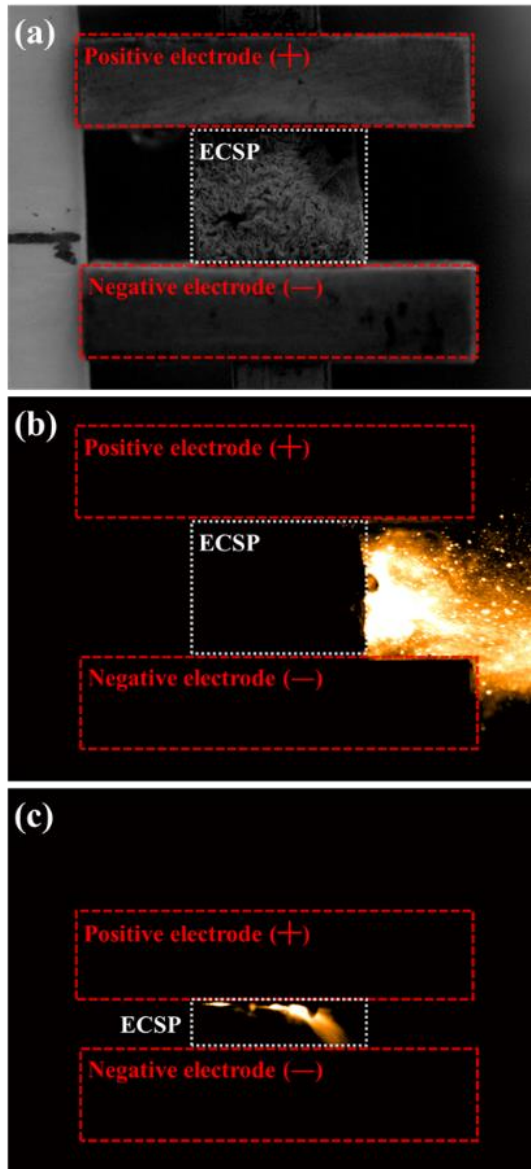


Figure 3: High-speed burning image of (a) unburnt ECSP, (b) ECSP at transient region, and (c) ECSP at steady region

Figure 4 shows the electric power signals during the burning of M5 and M15. The burning region with change in electric power for M5 and M15 are referred as A-B-C and A'-B'-C', respectively. It is observed that in the transient region of M5 (A-B) and M15 (A'-B') follows similar trend showing almost same electric power. While, in the steady region, the trend shows a higher electric power for M5 (B-C) in comparison to M15 (B'-C'). It is observed that the power applied to M5 increased faster indicating high metal content propellant needs more electric power to achieve

steady burning.

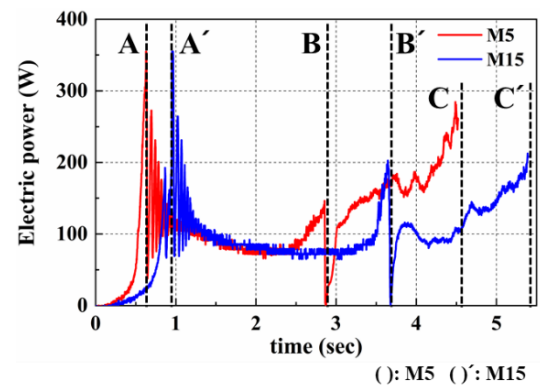


Figure 4: Electric power signals of M5 and M15.

### 3.2 Flame temperature

At steady burning region, the flame temperature was measured at 1.51 mm above the bottom of metal sample. Figure 5 shows the measured flame temperature for M5 and M15 at steady burning region. The average temperature was about 1788 K for M5 and about 1630 K for M15. It is observed that, the 10% increase in tungsten in the ECSP composition causes 9% decrease in flame temperature. In qualitative perspective, there was higher temperature fluctuation for M5 is observed as compared to M15. These is due to addition of metal oxide oxidation. During the combustion process, some of W would be transformed into WO or WO<sub>2</sub> easily, due to its molecular bonding characteristics. When the W content became higher, more W molecules transformed into W-oxide. With higher metal oxide contents, more thermal energy is absorbed during the combustion process. In other words, it increases the specific heat capacity of the higher metal content ECSP. Thus, it is inferred that more stable combustion could be achieved in the propellant with higher metal content.

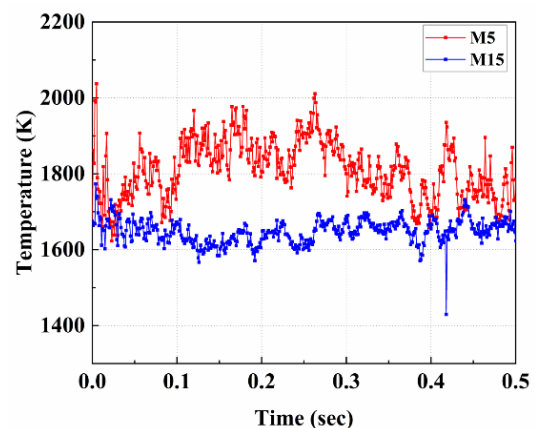


Figure 5: Flame temperature distribution of M5 and M15.

### 3.3 Decomposition characteristics

Figure 6 shows the DSC and TGA results of M5 and M15. The thermal analysis shows that the endothermic reaction occurred only before 100 °C and the remained water in the propellant was

evaporated. As soon as the endothermic reaction terminates, some portion of the exothermic reaction could be observed in 90-200 °C. Though most part of the exothermic reaction was occurred in the temperature range of 200-400 °C, some part of the decomposition process also takes place in this range. Here, the glycerol was decomposed dominantly, due to its decomposition property. About 191.3 °C (A'), exothermic reaction of M15 began to occur. Compared to the reaction of M5 (A-B,  $\Delta T=111.40^{\circ}\text{C}$ ), the decomposition of M15 (A'-B',  $\Delta T=174.65^{\circ}\text{C}$ ) occurs in the wide range of temperature. The reason for this difference could be formation of metal oxides. If the propellant includes higher metal content, there might be requested to apply higher energy to decompose, due to the increase of the bond in molecular level.

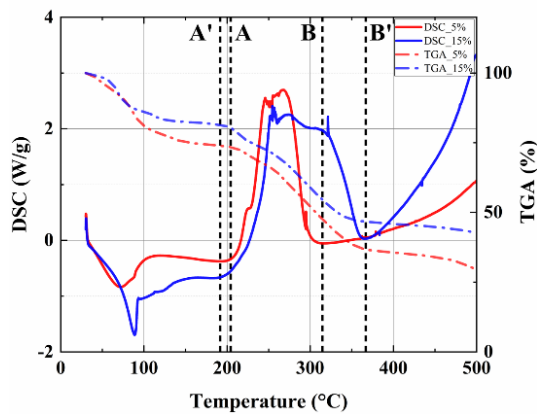


Figure 6: Thermal analysis results of M5 and M15.

## 4 Conclusions

In this study the combustion characteristics of M5 and M15 ECSPs were investigated using different measurement techniques, such as electric signal measurement, optical pyrometry, high-speed imaging, and thermal analysis. The overall burning process are classified into two regions, i.e. the transient and steady region based on the burning trend and electric signal. In the transient region, the internal current maintained constant, and the intermittent burning without decrease of propellant length was dominant. This burning mainly occurred on the front and rear surface, not on the interface between the propellant and positive electrode. However, in the steady region the internal current increased linearly, and with a consistent flame in between the interface of positive electrode and sample was observed. At the steady region, the differences between M5 and M15 could be clearly found out in terms of electric power and flame temperature. Further, it is observed that more the metal content in ECSP, higher the electric power required for burning the propellant. A 9% decrease in flame temperature was observed with the 10% increase in metal content (M15). The thermal analysis reveals, due to higher tungsten content in ECSP, the major exothermic reactions occurred in about 56% wider range in M15, while the difference of endothermic reaction was not significant.

## 5 Acknowledgment

This work was financially supported by the National Research Foundation of Korea (NRF-0498-20210020), contracted through IAAT and IOER at Seoul National University.

## References

- [1] C. Dennis, B. Bojko, *Fuel* 254 (2019) 115646.
- [2] W. Sawka, M. McPherson, *Electrical Solid Propellants: A Safe, Micro to Macro Propulsion Technology*, 49<sup>th</sup> ALAA/ASME/SAE/ASEE Jt. Propuls. Conf. (2013) 2013-4168.
- [3] M.S. Glascock, J.L. Rovey, K.A. Polzin, *Aerosp.* 7.6 (2020) 70.
- [4] I. Zamir, M. Ben-Reuven, A. Gany, D. Grinstein, *Propellants, Explos. Pyrotech.* 46.3 (2021) 477-483.
- [5] B. Gobin, N. Harvey, G. Young, *Combust. Flame* 244 (2022) 112291
- [6] L. Bao, H. Wang, Z. Wang, H. Xie, S. Xiang, X. Zhang, W. Zhang, Y. Huang, R. Shen, Y. Ye, *Combust. Flame* 236 (2022) 111804.
- [7] Z. He, Z. Xia, J. Hu, L. Ma, Y. Li, J. *Therm. Anal. Calorim.* 139.3 (2020) 2187-2195.
- [8] A.T. Hiatt, R.A. Fredric Jr, *Laboratory experimentation and basic research investigating electric solid propellant electrolytic characteristics*, 52<sup>nd</sup> ALAA/SAE/ASEE Jt. Propuls. Conf. (2016) 4935.
- [9] K. Gnanaprakash, M. Yang, J.J. Yoh, *Combust. Flame* 238 (2022) 111752.
- [10] Y. Li, Z. Xia, J. Hu, L. Ma, X. Na, Z. He, *Acta Astronaut.* 184 (2021) 167-179.
- [11] M.R. Weismiller, J.G. Lee, R.A. Yetter, *Proc. Combust. Inst.* 33.2 (2011) 1933-1940.